VOL. 4, NO. 2, APRIL 2009 ISSN 1819-6608
ARPN Journal of Engineering and Applied Sciences


www.arpnjournals.com

# COMPUTATIONAL MODELING AND SIMULATION OF LOW VELOCITY IMPACT ON FIBROUS COMPOSITE PANELS DROP_WEIGHT UN_PARTITIONED MODEL

Umar Farooq and Karl Gregory
Department of Product Design and Engineering, University of Bolton, United Kingdom
E-Mail: adalzai3@yahoo.co.uk and k.r.gregory@bolton.ac.uk

**ABSTRACT**

A computational model was developed to simulate and predict failure response of fibrous composite panels subjected to drop-weight impact on un-partitioned fibrous composite panels using finite element analysis.

The mathematical formulation consisting of constitutive, equilibrium, and strain-displacement relations; finite element formulation with contact and external forces; failure criteria proposed by Hashin. Finite Element Method (FEM) was chosen to perform simulation in commercially available software ABAQUS incorporating dynamic load in time-domain instead of using conventional analysis procedures of quasi-static indentation or drop weight model. To improve convergence, adaptive meshing techniques were employed to mesh the regions of high stress gradient with fine meshes and coarse meshes for the rest.

Results were compared with the results from the available literature and found to be in good agreement. However, some values of acceleration parameters were very large. That was due to being computed from second order derivates, divided by very small time step size produced such larger values. Therefore, a four-point moving average filter was applied to remove 'noise' from the results. Some of the results from failure threshold loads were selected and included in the form of tables, contour plots and graphs.

**Keywords**: finite element analysis, composite plates, failure criteria, delamination.

## INTRODUCTION

Advanced fibrous composites are being used in many advanced structural applications. Many of these structures are situated such that they are susceptible to foreign object impacts and in-plane loadings which cause invisible extensive damage. The damage can significantly reduce load bearing capability or cause catastrophic failures. Thus there exists the need to investigate the incurred damage to be able to improve tolerance of structures.

Due to the complicated interaction of different global, local and torsional buckling; damage mechanisms of fibre-matrix de-bonding, matrix cracking, fibre cracking, and de-lamination etc., no generally applicable methods for the analysis could have been established. Most of the available literature is experimental with little discussion on local buckling. Some of the relevant studies are given below.

The dynamic response of composite structures subjected to transient dynamic loading has been studied in terms of analytical, numerical (Aslan, 2006) and experimental works (Krishnamurthy, 2003). Pierson and Vaziri (1995) presented an analytical model based on the combined effects of shear deformation, rotary inertia and nonlinear Hertzian contact law with an aim of studying the low-velocity impact response of simply supported laminated composite plates. Sun in (1977) applied a modified Hertzian contact law to study low-velocity impact response analysis of composite laminates.

Yang and Sun (1981) presented the experimental indentation law through static indentation tests on composite laminates. Tam and Sun (1982) developed their own finite element program to analyze impact response of composite laminates and they performed impact tests using a pendulum type low-velocity impact test system. Ik Hyeon Choi and Cheol Ho Lim (2002) proposed a linearized contact law in studying low-velocity impact analysis of composite laminates and compared it to the modified Hertizan contact law (1983). sun and Chattopadhyay, Dobyns (1981) and Ramkumar and Chen (1983) employed the first-order shear deformation theory developed by Whitney and Pagano (1970) in conjunction with the Hertzian contact law to study the impact of laminated composite plates. Sankar (1982) presented a semi-empirical formula in predicting impact characteristics such as the peak force, the contact duration, and the peak strain on the back surface of laminates. Ganapathy and Rao (2001) predict the damage in laminated composite plates and in cylindrical/spherical shell panels subjected to low velocity impact. The continuity of the work conducted by the authors Tiberkak *et al.* (2005).

Gaussian points via our numerical model, and then the failure criterion suggested by Choi and Chang (2002) is used to predict matrix cracking and delamination. Impact Damage Resistance and Damage Tolerance of Fibre Reinforced Laminate Composites were investigated by Ritz in his PhD thesis (James, 2006). Tita, V., *et al.*, reported experimental and numerical approaches in their paper (Tita, 2008); however the numerical approach uses fracture mechanics for failure mechanism and prediction.

In the past most of the research on the topic has been experimental. Most of the work was focusing on

developing the phenomenological and the semi-analytical models by making appropriate assumptions based on the experimental observations. Therefore, a suitable computational model is essential to exploit the full benefits of the advanced composites.

Hence, the problem was transformed into numerical model to obtain adequate, consistent and reliable results. Moreover, an incidental or drop tool may not always impact the panel with a conventional hemisphere impactor, blunt-nozed object are also very common. Therefore, results from blunt/flat noze shape impactor were selected.

**Governing equations for laminates**

From classical laminate plate theory, the extensional stiffness matrix [*A*] relates the in-plane forces {*N*} to the mid-plane strains $\{\varepsilon^{o}\}$ and the bending stiffness matrix [D] relates the moments {M} to the curvatures $\{\kappa\}$. The coupling stiffness matrix [B] couples the in-plane forces {N} with the curvatures {κ} and the moments {*M*} with the mid-plane strains $\{\varepsilon^{o}\}$. Where $(Q_{ij})_h$ is the reduced stiffness for layer *h*, which is a function of the layer angle, $\theta_h$, and the layer in-plane orthotropic engineering constants, E's and $\nu$'s. $Z_h$ and $Z_{h-1}$ are the *Z* co-ordinates of the top and bottom surfaces of the *h* layer respectively. Considering a laminate made of "N" layers (lamina) of thickness "t" arranged as shown below. The integral can be replaced by a summation over all N layers.

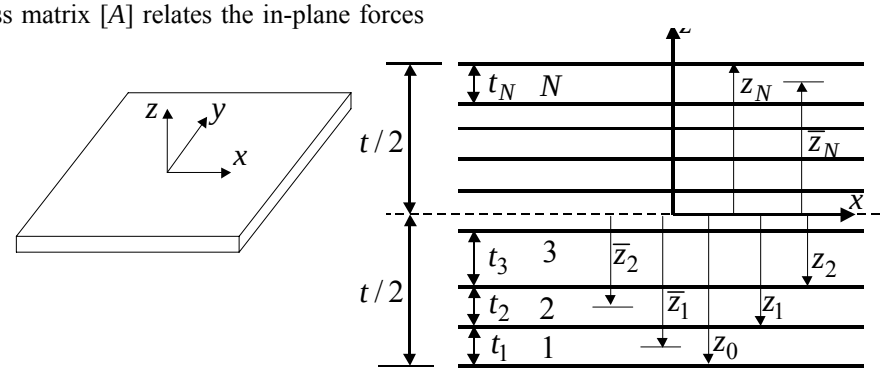


**Figure-1:** Laminate and plies lay-up through-the-thickness stacking.

Where k is the layer number counting from the bottom up, N is the number of layers in the laminate, and $z_k$ is the coordinate of the top surface of the $k^{th}$ layer. Both the mid-surface strains {$\varepsilon_{xo}$, $\varepsilon yo$, $\varepsilon_{xy0}$} and curvatures {K) are independent of z for the laminated plate, i.e., the mid-surface strains are at the laminated plate mid-surface (z = 0) and the curvature of each lamina is the same. For laminates the stresses can be written as:

$$\begin{Bmatrix}\sigma_1\\ \sigma_2\\ \sigma_6\end{Bmatrix}^k = \begin{bmatrix}Q_{11} & Q_{12} & 0\\ Q_{12} & Q_{22} & 0\\ 0 & 0 & Q_{66}\end{bmatrix}^k \begin{Bmatrix}\varepsilon_1\\ \varepsilon_2\\ \gamma_6\end{Bmatrix}^k$$

$$\begin{Bmatrix}\sigma_4\\ \sigma_5\end{Bmatrix}^k = \begin{bmatrix}Q_{44} & 0\\ 0 & Q_{55}\end{bmatrix}^k \begin{Bmatrix}\gamma_4\\ \gamma_5\end{Bmatrix}^k \quad (1)$$

The following laminate stiffness equations are obtained:

$$\begin{Bmatrix}N_x\\ N_y\\ N_{xy}\\ M_x\\ M_y\\ M_{xy}\end{Bmatrix}^k = \begin{bmatrix}A_{11} & A_{12} & A_{16} & B_{11} & B_{12} & B_{16}\\ A_{12} & A_{22} & A_{26} & B_{12} & B_{22} & B_{26}\\ A_{16} & A_{26} & A_{66} & B_{16} & B_{26} & B_{66}\\ B_{11} & B_{12} & B_{16} & D_{11} & D_{12} & D_{16}\\ B_{12} & B_{22} & B_{26} & D_{12} & D_{22} & D_{26}\\ B_{16} & B_{26} & B_{66} & D_{16} & D_{26} & D_{66}\end{bmatrix}^k \begin{Bmatrix}\varepsilon_x^0\\ \varepsilon_y^0\\ \gamma_{xy}^0\\ k_x\\ k_y\\ k_{xy}\end{Bmatrix}^k$$

$$\begin{Bmatrix}V_{yz}\\ V_{xz}\end{Bmatrix}^k = \begin{bmatrix}H_{44} & H_{45}\\ H_{45} & H_{55}\end{bmatrix}^k \begin{Bmatrix}\gamma_{yz}\\ \gamma_{xz}\end{Bmatrix}^k \quad (2)$$

Where the A, B and D coefficients are given by

$$A_{ij} = \sum_{k=1}^{N} \left(\overline{Q}_{ij}\right)_k \left(z_k - z_{k-1}\right) = \sum_{k=1}^{N} \left(\overline{Q}_{ij}\right)_k t_k \qquad i, j = 1, 2, 6$$

$$B_{ij} = \frac{1}{2}\sum_{k=1}^{N} \left(\overline{Q}_{ij}\right)_k \left(z^2{}_k - z^2{}_{k-1}\right) = \sum_{k=1}^{N} \left(\overline{Q}_{ij}\right)_k t_k z_k \qquad i, j = 1, 2, 6$$

$$B_{ij} = \frac{1}{2}\sum_{k=1}^{N} \left(\overline{Q}_{ij}\right)_k \left(z^2{}_k - z^2{}_{k-1}\right) = \sum_{k=1}^{N} \left(\overline{Q}_{ij}\right)_k t_k z_k \qquad i, j = 1, 2, 6$$

$$D_{ij} = \frac{1}{3}\sum_{k=1}^{N} \left(\overline{Q}_{ij}\right)_k \left(z^3{}_k - z^3{}_{k-1}\right) = \sum_{k=1}^{N} \left(\overline{Q}_{ij}\right)_k \left(t_k z_k^2 + \frac{t_k^3}{12}\right)_k \qquad i, j = 1, 2, 6$$

$$\begin{Bmatrix} V_x \\ V_y \end{Bmatrix} = \begin{bmatrix} H_{44} & H_{45} \\ H_{45} & H_{55} \end{bmatrix} \begin{Bmatrix} \gamma_{yx} \\ \gamma_{xz} \end{Bmatrix} \qquad H_{ij} = \frac{5}{4}\sum_{k=1}^{N}(\overline{Q}_{ij})_k \left[ t_k - \frac{4}{t^2}\left( t_k \overline{z}_k^2 + \frac{t_k^3}{12} \right) \right] \qquad i, j = 4,5 \quad (3)$$

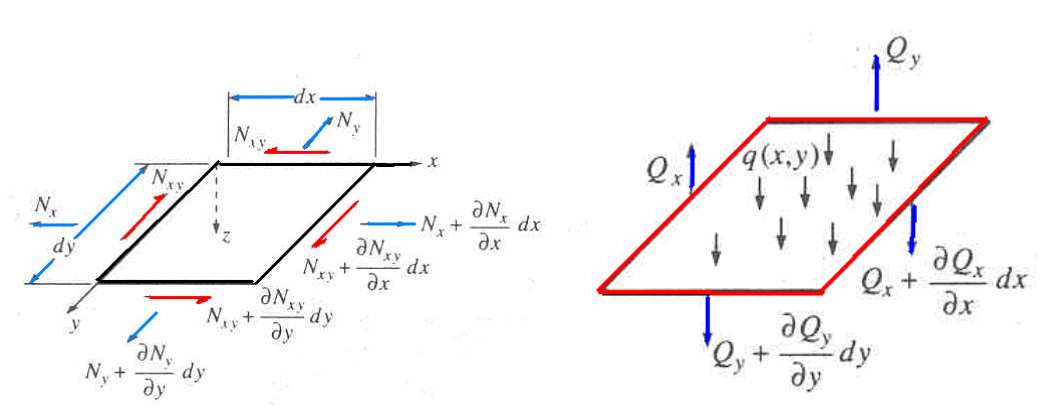


**Figure-2:** In-plane, out-of-plane, and uniformly distributed loads.

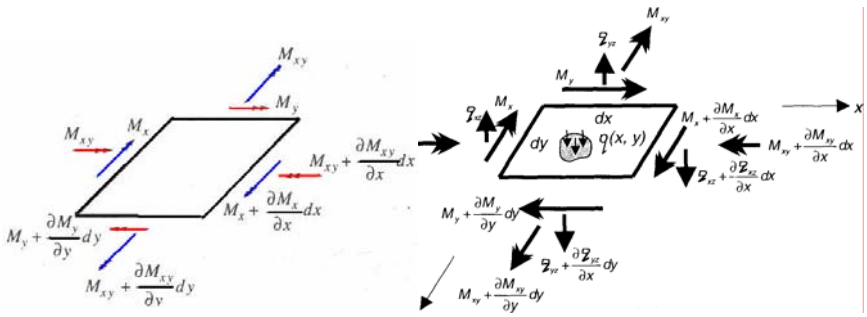


**Figure-3:** Moments and uniformly applied external load.

The summation of moments and forces in the z direction becomes:

$$\frac{\partial^2 M_x}{\partial x^2} + 2\frac{\partial^2 M_{xy}}{\partial x \partial y} + \frac{\partial^2 M_y}{\partial y^2} + N_x \frac{\partial^2 w}{\partial x^2} + 2N_{xy}\frac{\partial^2 w}{\partial x \partial y} + N_y \frac{\partial^2 w}{\partial y^2} + q(x,y) = 0 \qquad (4)$$

When the load is not uniformly distributed and shape of the impactor is point load applied at centre ($x_0$, $y_0$) then dirac delta function is

$$q(x_0, y_0) = P\delta(x - x_0)\delta(y - y_0) \qquad (5)$$

And for line and patch loads the Heaveside function will be used as follows.

$$q(x,y) = \int_{x_0-\alpha}^{x_0+\alpha} P\,\delta(x - x_0)dx \int_{y_0-\beta}^{y_0+\beta} \delta(y - y_0)dy \qquad (6)$$

These equations represent equilibrium for a laminate subjected to transverse uniformly distributed, point and patch loading. The equations are valid for isotropic as well as anisotropic or composite panels for plies at various rotations.

**The principal of virtual work**

The principal of virtual work for the model system can be written as

$$\int_V \{\delta u\}^T \rho \{\ddot{u}\} dV + \int_A [\{\delta \varepsilon^0\}^T \{N\} + \{\delta k\}^T \{M\}] dA - \int_S \{\delta u\}^T \{T\} dS + \delta w_i m \ddot{w}_i + F\delta\alpha = 0, \qquad (7)$$

The dynamic equation is given by:

$$[M]\{\ddot{u}\} + [K]\{u\} = \{F\}, \qquad (8)$$

Where [M] and [*K*] is, respectively, the mass matrix and stiffness matrix of the composites, given by

$$[M] = \sum \int_V [N]^T [\bar{m}][N] dV, \qquad (9)$$

Where

$$[\bar{m}] = \begin{bmatrix} I_1 & 0 & 0 & I_2 & 0 \\ 0 & I_1 & 0 & 0 & I_2 \\ 0 & 0 & I_1 & 0 & 0 \\ I_2 & 0 & 0 & I_3 & 0 \\ 0 & I_2 & 0 & 0 & I_3. \end{bmatrix},$$

Where,

$$(I_1, I_2, I_3) = \int_{-h/2}^{h/2} \rho(1, z, z^2)\, dz. \qquad (10)$$

**Hashin's failure criteria**

Interlaminar shear is one of the sources of failure in laminated plates. Since the interlaminar strength data are not usually available, some of the researchers have suggested using $\tau_{xz}$, = τy = $\tau_{Lt}$ and $\tau_{tz}$ = τt. With the use of the present theory, these stresses were calculated as follows:

$$\left(\sigma_{zz} \quad \tau_{xz} \quad \tau_{yz}\right) = \frac{1}{h}\int_0^z \left(\sigma_{zz} \quad \tau_{xz} \quad \tau_{yz}\right) dz \qquad (11)$$

The interlaminar shear stresses are then determined From the following equilibrium equations:

$$\tau_{yz} = \int_{\frac{-h}{2}}^{z} \left( \frac{\partial \sigma_y}{\partial y} + \frac{\partial \tau_{xy}}{\partial y} \right) dz \qquad (12)$$

Once the ply local stresses are known, it will be used in the following interaction equation of Hashin:

$$\left(\frac{\tau_{13}}{F_{su13}}\right)^2 + \left(\frac{\tau_{23}}{F_{su23}}\right)^2 = 1 \qquad (13)$$

Where $F_{su13}$ and $F_{su23}$ are the ultimate shear stresses,

**Numerical results and analysis**

The drop-weight model to predict the composites behaviour was implemented into ABAQUS™.

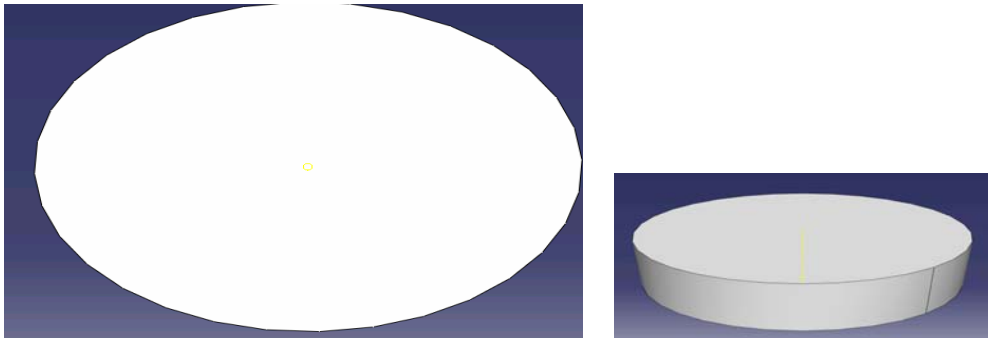

**Figure-4:** Schematic diagram of specimen and impactor.

Composite laminates of diameter 0.02394 m, with stacking sequences [45/0/-45/90] $_S$, [45/0/-45/90] $_{2S}$, and [45/0/-45/90] $_{3S}$ the effect of impact duration, length and position on the impact loads were studied with 0.00288 m thickness of quasi-isotropic configuration under centrally

Located load of 16 KN impact at circle of 0.0063 m diameter and length was 0.002 of aluminium was studied for various data input and stacking sequences and clamped boundary conditions. The properties of a unidirectional lamina of specimens with geometries and data are given in Table-1.

**Table-1:** Material properties used to develop specimen.

| **Material Properties GPa** | **Ultimate strengths MPa** | **Stacking sequences** |
|---|---|---|
| $E_1 = 150$; $E_2 = E3 = 15$ | $\left(\sigma_1^T\right)_{ult} = \left(\sigma_1^C\right)_{ult} = 1500$ | [45/0/-45/90] $_S$, [45/0/-45/90] $_{2S}$, |
| $G_{12} = 5.7$ $G_{13} = 5.7$; $G23 = 7.26$ | $\left(\sigma_2^T\right)_{ult} = 40$ $\left(\sigma_2^C\right)_{ult} = 20$ | |
| Poisson's Ratios $\nu_{12} = 0.33$; $\nu_{23} = 0.03$; $\nu_{13} = 0.01$ | $\left(\tau_{12}\right)_{ult} = \left(\tau_{12}\right)_{ult} = 53$ | [45/0/-45/90] 3S |

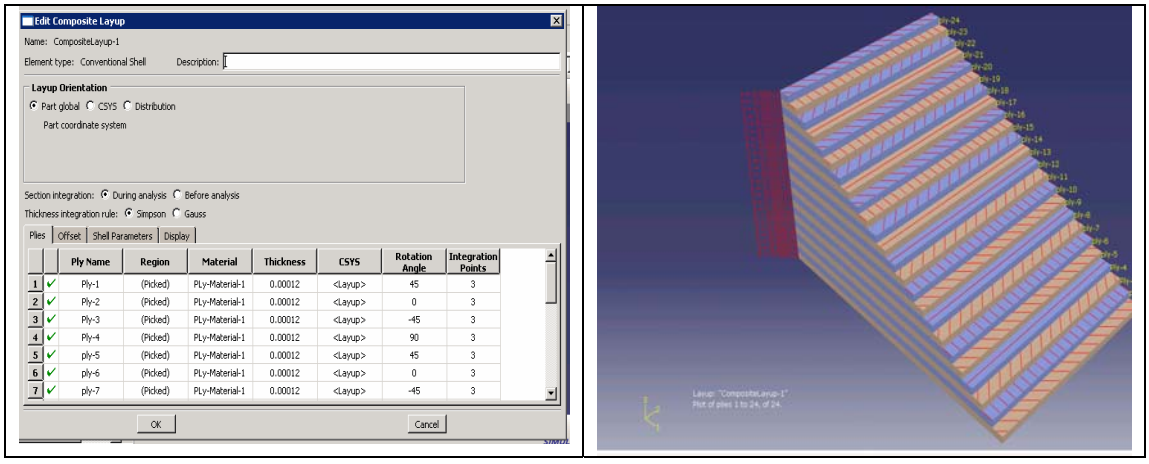


**Table-2 and Figure-5:** Input data and stack of 24 un-symmetric plies.

The circular disk and impactor were used in a clamped set-up under a load applied at the centre, shown in the Figure-6 below.

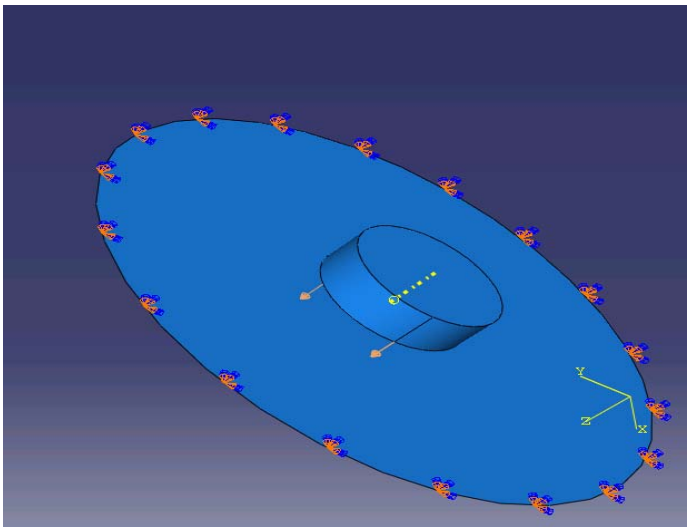

**Figure-6:** Model after applying load and boundary conditions.

Meshing using finite elements: (a) shell element S4 and (b) solid element C3D8 for impactor were created see Figure-7 below.

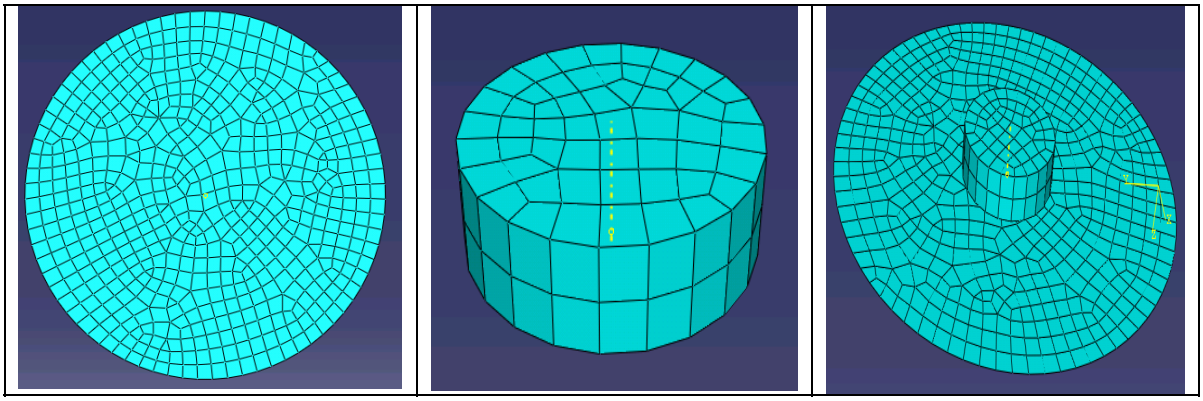

**Figure-7:** Meshed specimen, impactor, and the model.


Given the fixed ply thickness for the material results for acceleration, velocity, displacements, stresses and strains were computed. The time duration was considered 1.1 μsec for which amplitudes of velocities were used to impact the models. The predicted results were used in Hishon criteria and FPF was achieved with degradation of properties by the weight-drop.

Computed values for accelerations were very large and confusing as values were obtained from second-order derivative, in such cases even rounding off numbers in the intermediate steps can lead to considerable errors in the final results. Therefore a four-point moving average filter was applied to remove and reduce the noise of computation errors.

**Table-3:** Time versus amplitudes of velocities.

| **Time Sec x $10^{-3}$** | | | **Velocity -5 m/sec** | | |
|---|---|---|---|---|---|
| 0 | Amp 1 | Amp2 | Amp 3 | Amp 4 | Amp 5 |
| 0.055 | 0.05 | 0.05 | 0.02 | 0.05 | 0.05 |
| 0.11 | 0.08 | 0.05 | 0.02 | 0.1 | 0.1 |
| 0.165 | 0.15 | 0.06 | 0.03 | 0.2 | 0.1 |
| 0.22 | 0.3 | 0.1 | 0.04 | 0.3 | 0.1 |
| 0.275 | 0.4 | 0.2 | 0.05 | 0.4 | 0.1 |
| 0.33 | 0.5 | 0.3 | 0.1 | 0.5 | 0.2 |
| 0.385 | 0.6 | 0.4 | 0.2 | 0.6 | 0.2 |
| 0.44 | 0.7 | 0.5 | 0.3 | 0.7 | 0.2 |
| 0.495 | 0.8 | 0.6 | 0.4 | 0.8 | 0.3 |
| 0.55 | 0.9 | 0.8 | 0.5 | 0.9 | 0.8 |
| 0.605 | 1 | 0.9 | 0.6 | 1 | 0.9 |
| 0.66 | 0.9 | 1 | 0.7 | 0.9 | 1 |
| 0.715 | 0.8 | 0.9 | 0.8 | 0.8 | 0.9 |
| 0.77 | 0.6 | 0.8 | 0.9 | 0.7 | 0.8 |
| 0.825 | 0.5 | 0.7 | 1 | 0.6 | 0.3 |
| 0.88 | 0.4 | 0.6 | 0.9 | 0.5 | 0.3 |
| 0.935 | 0.3 | 0.5 | 0.8 | 0.4 | 0.2 |
| 0.99 | 0.3 | 0.4 | 0.7 | 0.4 | 0.2 |
| 01.045 | 0.2 | 0.2 | 0.6 | 0.3 | 0.2 |
| 1.1 | 0.2 | 0.3 | 0.5 | 0.3 | 0.2 |

**Table-4:** Runs for each amplitude versus computed results.

| **Runs** | **Acceleration X $10^{3}$ m/sec$^2$** | **Displacement X $10^{-3}$ m** | **Velocity m/sec** | **Strain X $10^{-2}$** | **Stresses GPa** |
|---|---|---|---|---|---|
| 1 | -5.0 | -2.50 | 5 | 1.60 | 6.42 |
| 2 | 11 | -1.50 | 5 | 1.80 | 6.18 |
| 3 | 6. | -1.70 | 5 | 1.40 | 6.37 |
| 4 | 6. | 1.40 | 5 | 1.40 | 6.89 |
| 5 | 10 | 1.12 | 5 | 1.40 | 4.79 |

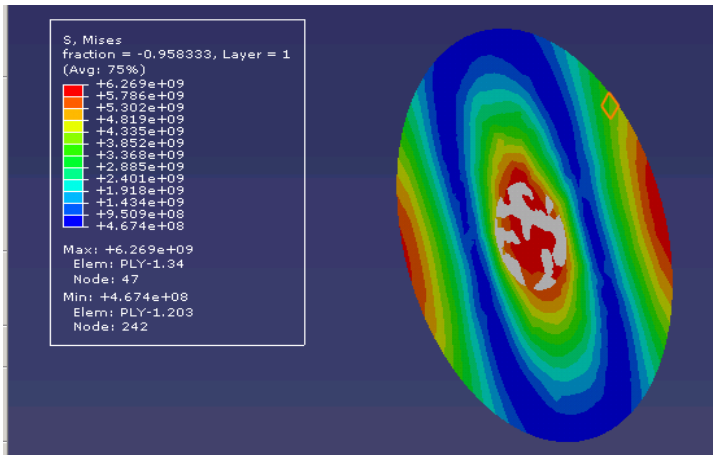


**Figure-8:** Images of principal stresses in $S_{11}$ directions.

The images comparison demonstrates that the computation of the inter-laminar shear stresses and peel stress in the links were realistic.

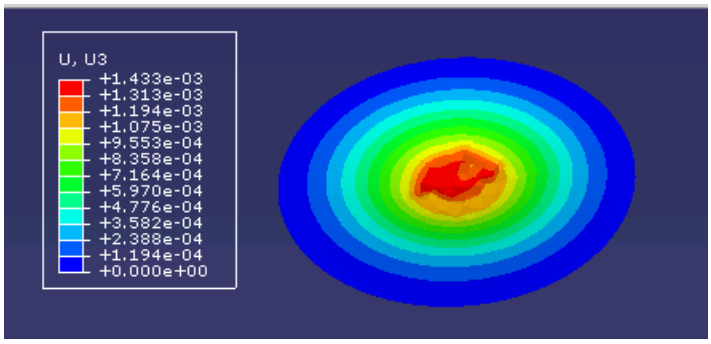


**Figure-9:** Images of out-of-plane displacements.

The images comparison demonstrates that the displacement values are within limits, according to the expectation and were realistic.

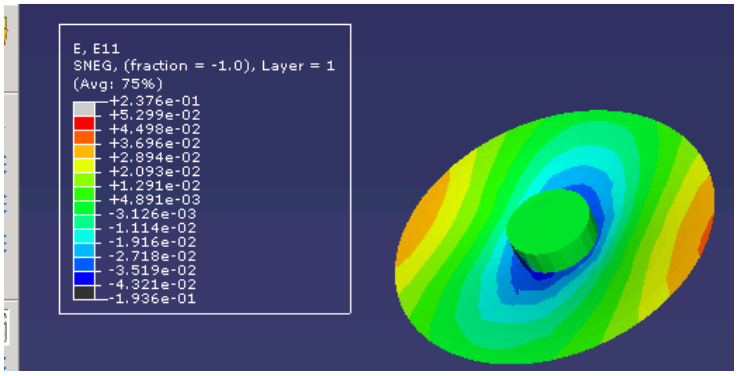


**Figure-10:** Images of principal strains in $X_{11}$ directions.

The images comparison demonstrates that the computation of the strain values were within the expected range and were realistic.

### 3 Graphs

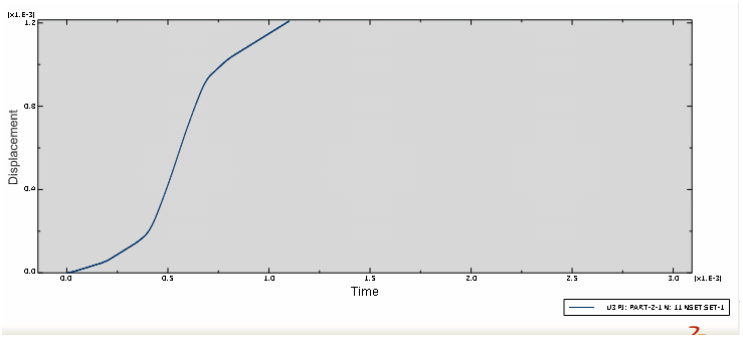


**Graph-1:** Graphics of displacements.

The graphs comparison demonstrates that the computation of displacement values were realistic.

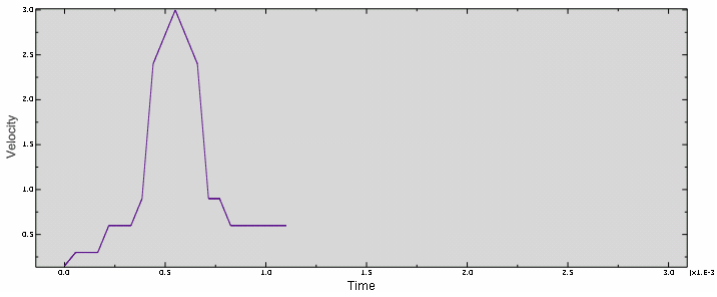


**Graph-2:** Velocities graphs.

The graphs comparison demonstrates that the computation of the velocities were realistic.

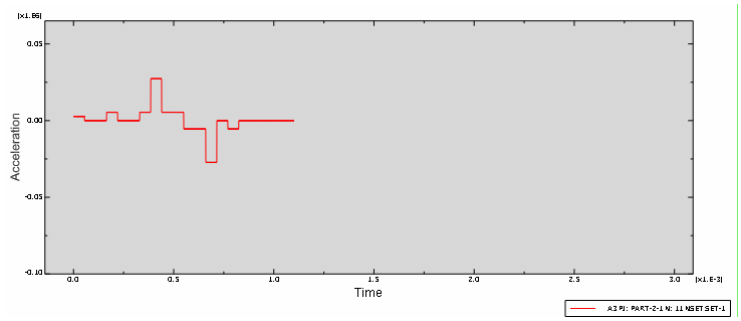


**Graph-3:** Graph of acceleration values.

The graphs comparison demonstrates that the computation of the acceleration were realistic.

## CONCLUSIONS

The laminate stress and strength analysis under drop-weight model has been illustrated successfully. The model is capable to simulation impact phenomena of various noze shapes of impactors. However, simulations from flat noze shape impactors were selected. Numerical predictions gave consistently good results, which means that FE code and the panel models are adequate and reliable.

Computed values of the principal stresses were compared with the allowable stresses against the given values and Hashin's failure criterion to predict FPF. The results matched and agreed well against the criteria as expected. If the load further increased the damaged areas further increase as well that may lead to de-lamination growth and failure.

In some cases, even rounding off numbers in the intermediate steps can lead to considerable errors in the final results. Therefore, great care was exercised in such calculations for accurate results.

In general terms, the present study has demonstrated the important contribution of blunt shape object/impactor resulting damage and response of composite panels. The predicted results can be used in design development as they have also validated the strategies of experimental models.


**REFERENCES**

[1] ABAQUS Users Manual, Version 6.6, ©2006 ABAQUS. Inc.

[2] Aslan Z., Karakuza, R., and Okutan B. 2003. The response of composites under low-velocity impact Compos Struct. 59. pp. 119-127.

[3] Dobyns A.L. 1981. Analysis of simply supported orthotropic plates subjected to static and dynamic loads AIAA J. 19. pp. 642-650.

[4] James R. A. 2006. Impact Damage Resistance and Damage Tolerance of Fibrous Composites PhD thesis. University of Bolton, UK.

[5] Krishnamurthy K.S., Mahajan, P., and Mittal R. K. 2003. Impact response and damage in composite cylindrical shells. Compos Struct. 59. pp. 15-36.

[6] Li C.F., Hu, N., Yin, Y.J., Sekine, H. and Fukunaga H. 2002. Low-velocity impact damage of composites. Part I an FEM model. Comp. pp.1055-1062.

[7] Mili F. and Necib B. 2001. Impact behavior of cross-ply composites under low velocities Compos Struct. 51. pp. 237-244.

[8] Naidu N. V. S. and Sinha P.K. 2005. Nonlinear finite element analysis of shells in hygrothermal environments Compos Struct. 69. pp. 387-395.

[9] Pierson M.O. and Vaziri R. 1995. Analytical solution for low-velocity impact response of composites AIAA J. 34. pp. 1633-1640.

[10] Ramkumar R. L. and Chen P.C. 1983. Low-velocity impact response of laminated plates AIAA J. 21. pp. 1448-1452.

[11] Sankar B.V. 1992. Scaling of low-velocity impact for symmetric composites J Reinf Plast Compos. 11. pp. 297-305.

[12] Sekine H., Hu, N., Fukunaga, H., and Natsume. 1998. T., Low-velocity impact response of composite Mech Compos Mater Struct. 5. pp. 275-278.

[13] Sun C.T. 1977. An analytical method for evaluation of impact damage [18] energy of composites Am Soc test mater ASTM STP. 617. pp. 427-440.

[14] Tam T. M., Sun C. T. 1982. Wave propagation in graphite/epoxy composites due to impact. NASACR 168057.

[15] Vaziri R., Quan, X., and Oslon M. D. 1996. Impact of composite plates and shells by super finite elements. Int J Impact Engng. 18(7-8): pp. 765-782.

[16] Whitney J.M. and Pagano N.J. 1970. Shear deformation in heterogeneous anisotropic plates ASME J Appl Mech. 37. pp. 1031-1036.

[17] Yang S.H. and Sun C.T. 1981. Indentation law for composites Am Soc Test Mater ASTM STP. 787. pp. 425-449.